Erratum: Proton-neutron multiplet states and isomers in the odd-odd nucleus ^{122}I [Phys. Rev. C 100, 024319 (2019)]

B. Moon, C.-B. Moon, G. D. Dracoulis, R. A. Bark, A. P. Byrne, P. A. Davidson, G. J. Lane, T. Kibédi, A. N. Wilson, and C. Yuan

(Received 15 April 2022; published 3 August 2022)

DOI: 10.1103/PhysRevC.106.029901

Since the original paper was published, a problem has come to our attention concerning the γ-ray energies and the level scheme. In the original published paper the level energies were determined by the strongest transitions and other connecting γ-ray energies were slightly adjusted to give agreement with the level energy differences. This is an inappropriate scientific procedure, in particular, because these γ-ray energies will enter into nuclear databases used by many scientists. The problem is particularly serious if, subsequently, a γ ray is discovered to be incorrectly placed either in this level scheme or if it belongs to another nucleus.

This Erratum, therefore, corrects the original paper by presenting new compilations with the actually measured γ-ray energies and uncertainties.

It is worth noting that Figs. 3, 6, 9 and 19 in the original paper are revised based on corrected energy values represented in Table I in this Erratum. A typographical error 907 keV in Fig. 24 is corrected as 927 keV.

In the **EXPERIMENTAl RESULTS AND LEVEL SCHEME** section (p. 3, right column):

Despite its excitation energy being unknown, two separate sequences of the **273-(351)-(375)-(405)**-keV and the **184-301-340-359-380-396**-keV transitions were found to feed the isomer. One can see that on one side, the **273**-keV-based sequence corresponds to band 7 and, on the other side, the **184**-, 301-, 340-, **359**-, **380**-, and **396**-keV peaks are members of band 1 from the 16^+ state at 3008-keV to the 8^+ states at **394** keV.

In the **EXPERIMENTAl RESULTS AND LEVEL SCHEME** section (p. 9, left column):

We assigned this band-head at **731** keV as 5^+ according to the observation of the similar bands in ^{124}I [9] and ^{126}I [9].

In the **EXPERIMENTAl RESULTS AND LEVEL SCHEME** section (p. 10, left column):

Let us explain more details regarding the existence of the triple 8^+ states at 786, **389**, and 394 keV. The **389**-keV level fed by both the 396- and 776-keV transitions has the following features; first, there is no observation of transitions depopulating this level.

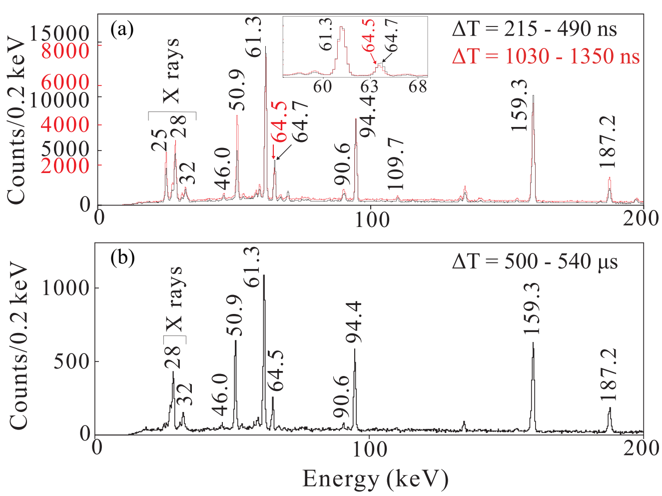

FIG. 3. Delayed singles γ-ray spectra from the ^{120}Sn(^{7}Li, $5n$) reaction at 58 MeV under varied beam off conditions ΔT. (a) For the beam on and off, 1 ns–1.7 μs, measurements; ΔT = 215–490 ns is the black line and ΔT = 1030–1350 ns is the dotted red (gray) line. (b) For the beam on-beam off, 60–880 μs, measurements; ΔT = 500–540 μs. Note the difference in energies between the 64.5-keV and the 64.7-keV peaks and the difference in relative intensities in the 51-keV transitions. In (a) the inset represents the separated spectra of the 64.5- and 64.7-keV double peaks where the 64.5-keV transition indicates a decaying transition from a longer isomer than an associated isomer with the 64.7-keV transition. Note that all energy values are corrected based on Table I.

The changes from the published paper are in all cases small, and the physics conclusionarrived at previously are not changed.

TABLE I. γ-ray energies, relative intensities, directional correlation of oriented state (DCO) values, multipolarities of the transitions belonging to ^{122}I, together with spin assignments of the initial and final levels. Isomeric states include their half-lives. Corrected γ-ray and level energies are noted with asterisk marks.

E_i (keV)[a]	E_f (keV)[a]	E_γ (keV)[a]	I_γ (%)[b]	DCO[c]	Multipolarity	$J_i^\pi \to J_f^\pi$	Half-life
Low-lying states							
61.3	0	61.3	60(1)		$M1$	$2^+ \to 1^+$	
90.6	0	90.6	2(0.6)				
109.7	0	109.7	4(1)				
109.7	90.6	19.1					
155.7	61.3	94.4	40(1)	0.91(3)[1], 1.14(2)[3]	$E2$	$4^+ \to (2^+)$	16.6(2) ns
155.7	109.7	46.0	1(1)				
315.0	155.7	159.3	100	0.74(2)[1], 0.97(1)[3]	$E3$	$7^- \to 4^+$	193.3(9) ns
342.9	155.7	187.2	11(2)	1.05(12)[1]	$E2$	$(6^+) \to 4^+$	
342.9	315.0	27.9					
379.5	315.0	64.5	19(2)		$M1/E2$	$7^- \to 7^-$	79.1(12) μs
393.8*	342.9	50.9*	18(2)		$E2$	$(8^+) \to (6^+)$	78.2(4) μs
458.4	315.0	143.4	60(2)	0.72(1)[1], 0.73(1)[1]	$M1/E2$	$8^- \to 7^-$	
519.3	315.0	204.3	49(2)	0.54(2)[1]	$M1/E2$	$8^- \to 7^-$	
534.7*	315.0	219.7*	1(0.7)				
785.4*	389.1*	396.3*	56(4)	0.94(4)[1], 1.19(4)[3]	$M1/E2$	$(8^+) \to (8^+)$	
785.4*	393.8*	391.6*	38(3)	1.06(5)[1], 1.00(7)[3]	$M1/E2$	$(8^+) \to (8^+)$	
787.1*	315.0	471.4*	2(1)			$8^- \to 7^-$	
787.1*	534.7*	253.1*	2(1)				
1017.2*	315.0	702.1	31(4)				
1017.2*	458.4	558.8*	11(4)				
1017.2*	519.3	497.8	8(2)	0.42(15)[1]			
1091.9	315.0	776.9	5(1)				
1091.9	458.4	633.5					
1165.9*	389.1*	776.5	33(4)	1.00(3)[1], 1.48(5)[3]	$E2$	$10^+ \to (8^+)$	
1165.9*	393.8*	772.9*	20(3)	0.95(5)[1], 1.16(7)[3]	$E2$	$10^+ \to (8^+)$	
1165.9*	746.1*	419.9*	20(3)	0.67(4)[1]		$10^+ \to 9^-$	
1165.9*	785.4*	379.9*	76(3)	1.20(5)[1], 1.28(3)[3]	$E2$	$10^+ \to (8^+)$	
1165.9*	1017.2*	148.8*	13(3)	0.60(8)[1]		$10^+ \to (9^-)$	
1165.9*	1091.9	74.2	7(2)			$10^+ \to (9^-)$	
Band1							
1535.8*	1165.9*	369.9*	32(2)	0.55(2)[1]	$M1/E2$	$11^+ \to 10^+$	
1824.2*	1165.9*	658.9	92(3)	1.18(2)[1], 1.48(2)[3]	$E2$	$12^+ \to 10^+$	
1824.2*	1535.8*	287.8*	10(2)	0.52(3)[1]	$M1/E2$	$12^+ \to 11^+$	
2183.9*	1535.8*	648.6*	12(1)	0.91(5)[1]	$E2$	$13^+ \to 11^+$	
2183.9*	1824.2*	359.2*	38(3)	0.48(5)[1]	$M1/E2$	$13^+ \to 12^+$	
2523.3*	1824.2*	699.0*	52(2)	1.11(3)[1]	$E2$	$14^+ \to 12^+$	
2523.3*	2183.9*	339.5*	15(2)	0.47(6)[1]	$M1/E2$	$14^+ \to 13^+$	
2823.7*	2183.9*	639.6*	27(1)	0.95(7)[1]	$E2$	$15^+ \to 13^+$	
2823.7*	2523.3*	300.5*	35(2)	0.46(2)[1], 0.70(3)[3]	$M1/E2$	$15^+ \to 14^+$	
3007.7*	2523.3*	484.4*	10(2)	0.93(5)[1]	$E2$	$16^+ \to 14^+$	
3007.7*	2823.7*	183.9	34(1)	0.54(2)[1], 0.73(2)[3]	$M1/E2$	$16^+ \to 15^+$	
3596.8*	2523.3*	1073.5*	1(0.7)		$E2$	$16^+ \to 14^+$	
3948.7*	2823.7*	1125.6*	2(1)		$E2$	$17^+ \to 15^+$	
3948.7*	3007.8*	941.8*	2(1)	0.57(10)[1]	$M1/E2$	$17^+ \to 16^+$	
3948.7*	3596.8*	350.5*	1(0.7)		$M1/E2$	$17^+ \to 16^+$	
4216.6*	3948.7*	267.6*	3(1)		$M1/E2$	$18^+ \to 17^+$	
4216.6*	3007.7*	1209.2	19(2)	0.96(4)[1], 1.40(8)[3]	$E2$	$18^+ \to 16^+$	
5143.5*	4216.6*	926.9*	17(1)	1.15(4)[1], 1.55(5)[3]	$E2$	$20^+ \to 18^+$	
5492.0*	5143.5*	348.5*	8(1)	1.08(5)[1]	$E2$	$22^+ \to 20^+$	
6215.3*	5492.0*	723.3*	7(1)	0.78(8)[1]	$M1/E2$	$23^+ \to 22^+$	
7021.8*	6215.3*	806.5*	5(1)	0.87(11)[1]	$E2$	$25^+ \to 23^+$	
8321.5*	7021.8*	1299.7	2(1)	1.06(17)[1]	$E2$	$27^+ \to 25^+$	

TABLE I. (*Continued.*)

E_i (keV)[a]	E_f (keV)[a]	E_γ (keV)[a]	I_γ (%)[b]	DCO[c]	Multipolarity	$J_i^\pi \rightarrow J_f^\pi$
Band2						
1209.1	519.3	689.8	< 1		$M1/E2$	$9^- \rightarrow 8^-$
1774.7*	787.1*	986.6*	< 1		$E2$	$10^- \rightarrow 8^-$
1774.7*	1017.2*	758.4*	4(1)	0.51(25)[1]	$M1/E2$	$10^- \rightarrow 9^-$
1774.7*	1108.5*	666.4	1(0.7)	1.10(35)[1]	$M1/E2$	$10^- \rightarrow 10^-$
2013.2*	1209.1	804.0*	2(1)		$E2$	$11^- \rightarrow 9^-$
2013.2*	1774.7*	238.5			$M1/E2$	$11^- \rightarrow 10^-$
2333.7*	1535.8*	798.9*			$E1$	$12^- \rightarrow 11^+$
2333.7*	1774.7*	558.8	6(2)	0.88(5)[1]	$E2$	$12^- \rightarrow 10^-$
2333.7*	2013.2*	319.7*	1(0.6)		$M1/E2$	$12^- \rightarrow 11^-$
2649.1*	2013.2*	636.6			$E2$	$13^- \rightarrow 11^-$
2649.1*	2333.7*	314.7*			$M1/E2$	$13^- \rightarrow 12^-$
2988.2*	2183.9*	803.6	1(1)	0.76(21)	$E1$	$14^- \rightarrow 13^+$
2988.2*	2333.7*	654.7*	11(3)	0.91(7)[1]	$E2$	$14^- \rightarrow 12^-$
2988.2*	2649.1*	339.5*			$M1/E2$	$14^- \rightarrow 13^-$
3407.0*	2649.1*	758.3*			$E2$	$15^- \rightarrow 13^-$
3407.0*	2988.2*	418.3			$M1/E2$	$15^- \rightarrow 14^-$
3774.4*	2823.7*	949.9*	1(1)	0.55(12)	$E1$	$16^- \rightarrow 15^+$
3774.4*	2988.2*	786.4*	21(3)	0.96(2)[1]	$E2$	$16^- \rightarrow 14^-$
3774.4*	3407.0*	368.0			$M1/E2$	$16^- \rightarrow 15^-$
3774.4*	3640.6*	133.7			$M1/E2$	$16^- \rightarrow 16^-$
4205.6*	3407.0*	798.9*			$E2$	$17^- \rightarrow 15^-$
4205.6*	3774.4*	431.1*			$M1/E2$	$17^- \rightarrow 16^-$
4517.8*	3774.4*	743.4*	14(3)	0.97(1)[1]	$E2$	$18^- \rightarrow 16^-$
4953.9*	4205.6*	748.3			$E2$	$19^- \rightarrow 17^-$
5220.3*	4517.8*	702.5*	10(2)	1.00(3)[1]	$E2$	$20^- \rightarrow 18^-$
5461.0*	5220.3*	240.7*	3(1)	0.46(4)[1]	$M1/E2$	$21^- \rightarrow 20^-$
6008.7*	5220.3*	788.2*	3(1)		$E2$	$22^- \rightarrow 20^-$
6008.7*	5461.0*	547.9	3(1)	0.65(5)[1]	$M1/E2$	$22^- \rightarrow 21^-$
Bands 3, 4, and 5						
746.1	458.4	287.8*	61(2)	0.59(1)[1], 0.69(2)[3]	$M1/E2$	$9^- \rightarrow 8^-$
746.1	519.3	226.8	28(1)	0.57(11)[1], 0.94(7)[2]	$M1/E2$	$9^- \rightarrow 8^-$
1108.5*	458.4	650.2*	30(1)	1.68(10)[2]	$E2$	$10^- \rightarrow 8^-$
1108.5*	746.1	362.2*		1.13(12)[2]	$M1/E2$	$10^- \rightarrow 9^-$
1244.4*	519.3*	725.6*	18(2)	1.57(13)[2]	$E2$	$10^- \rightarrow 8^-$
1244.4*	746.1	497.8*			$M1/E2$	$10^- \rightarrow 9^-$
1489.5*	746.1	743.4*	27(1)	1.84(9)[2]	$E2$	$11^- \rightarrow 9^-$
1848.9*	1068.0*	781.3			$E2$	$12^- \rightarrow 10^-$
1848.9*	1108.9	740.7	12(2)	0.91(8)[1], 1.89(26)[2]	$E2$	$12^- \rightarrow 10^-$
1848.9*	1443.0	405.4			$M1/E2$	$12^- \rightarrow 11^-$
1848.9*	1489.4	360.2			$M1/E2$	$12^- \rightarrow 11^-$
2071.8*	1244.9*	827.4	7(3)	1.09(37)[1], 1.93(29)[2]	$E2$	$12^- \rightarrow 10^-$
2356.0	1489.5*	866.5*	11(2)	1.06(8)[1], 1.94(14)[2]	$E2$	$13^- \rightarrow 11^-$
2679.0*	1840.5*	838.3			$E2$	$14^- \rightarrow 12^-$
2679.0*	1848.9*	830.6	6(2)	1.09(26)[1], 1.68(32)[2]	$E2$	$14^- \rightarrow 12^-$
2679.0*	2356.0	322.8*			$M1/E2$	$14^- \rightarrow 13^-$
3046.5*	2071.8*	974.7*	3(1)	1.77(51)[2]	$E2$	$14^- \rightarrow 12^-$
3342.6*	2356.0	986.6*	5(1)	1.12(10)[1], 1.95(41)[2]	$E2$	$15^- \rightarrow 13^-$
3640.6*	2679.0*	961.6	5(1)	1.25(35)[1], 2.70(37)[2]	$E2$	$16^- \rightarrow 14^-$
4167.0*	3342.6*	824.4*	1(0.5)	2.25(67)[2]	$E2$	$17^- \rightarrow 15^-$
4604.4*	3640.6*	963.8	2(1)	1.90(50)[2]	$E2$	$18^- \rightarrow 16^-$
Band 6						
1720.4*	1017.2*	702.5*				
1720.4*	1108.5*	612.5*		0.88(35)[2]		
2502.6*	1720.4*	782.2*		1.79(33)[2]		
3290.8*	2502.6*	788.2*				
4247.5*	3290.8*	956.7*				

TABLE I. (*Continued.*)

E_i (keV)[a]	E_f (keV)[a]	E_γ (keV)[a]	I_γ (%)[b]	DCO[c]	Multipolarity	$J_i^\pi \to J_f^\pi$
Band 7 and 8						
444.2	379.5	64.7	(1.9)	0.77(2)[4]	$M1$	$8^- \to 7^-$
717.2	444.2	273.0*	43(1)	0.97(2)[4], 0.94(3)[3]	$M1/E2$	$9^- \to 8^-$
1068.0*	444.2	624.1	8(1)		$E2$	$10^- \to 8^-$
1068.0*	717.2	350.5*	28(1)	0.98(2)[4]	$M1/E2$	$10^- \to 9^-$
1258.5*	444.2	814.3*	4(1)		$E2$	$10^- \to 8^-$
1258.5*	717.2	541.2*	5(2)	1.02(26)[4]	$M1/E2$	$10^- \to 9^-$
1443.0*	717.2	725.6*	8(1)	1.07(31)[4]	$E2$	$11^- \to 9^-$
1443.0*	1068.0	375.2*	13(2)	0.96(3)[4]	$M1/E2$	$11^- \to 10^-$
1623.0*	1068.0*	555.8*	<1	1.14(21)[4]	$M1/E2$	$11^- \to 10^-$
1623.0*	1258.5*	363.7		1.21(65)[4]	$M1/E2$	$11^- \to 10^-$
1840.1*	1068.0*	772.9*	7(1)	1.38(16)[4]	$E2$	$12^- \to 10^-$
1840.1*	1443.0*	396.3*	4(2)	1.28(12)[4]	$M1/E2$	$12^- \to 11^-$
2065.7*	1623.0*	443.3*	3(1)		$M1/E2$	$12^- \to 11^-$
2065.7*	1258.5*	806.5*	<1		$E2$	$12^- \to 10^-$
2271.6*	1443.0*	828.9	6(2)	1.30(27)[4]	$E2$	$13^- \to 11^-$
2271.6*	1840.1*	431.1*	2(1)	1.83(20)[4]	$M1/E2$	$13^- \to 12^-$
2544.7*	1623.0*	922.1	<1		$E2$	$13^- \to 11^-$
2544.7*	2065.7*	478.6*	2(1)		$M1/E2$	$13^- \to 12^-$
2728.1*	1840.1*	888.1		1.46(48)[4]	$E2$	$14^- \to 12^-$
2728.1*	2271.6*	456.4*	2(1)	0.72(38)[4]	$M1/E2$	$14^- \to 13^-$
3050.7*	2544.7*	506.0	<1		$M1/E2$	$14^- \to 13^-$
3215.2*	2271.6*	943.7*	2(1)	1.25(37)[4]	$E2$	$15^- \to 13^-$
3215.2*	2728.1*	487.0*	<1		$M1/E2$	$15^- \to 14^-$
3672.2*	3215.2*	456.4*			$M1/E2$	$16^- \to 15^-$
3672.2*	2728.1*	944.7*			$E2$	$16^- \to 14^-$
L1, L2, and band 9						
154.4	109.7	44.7				
162.3*	90.6	71.7*				
176.8	154.4	22.4				
176.8	162.3*	14.5*				
246.5*	109.6*	137.0				
246.5*	154.4	91.7*				
246.5*	162.3*	84.4*				
299.4	176.8	122.7*				
299.4	246.5*	52.7				
357.4*	155.7	201.7*				
452.7*	299.4	153.3*				
502.8*	357.4*	145.4				
581.7*	342.9	238.5*				
581.7*	502.8*	79.2				
731.3*	452.7*	278.6				
858.1*	581.7*	276.4				
1428.8*	731.3*	697.5			$E2$	$(7^+) \to (5^+)$
2187.2*	1428.8*	758.4*			$E2$	$(9^+) \to (7^+)$

[a]Energies are accurate ±0.3 keV.
[b]Normalization to 100 for the 159-keV transition.
[c]1; stretched quadrupole gate, 2; stretched dipole gate, 3; total DCO projection, 4; 273–351 dipole sum gate.

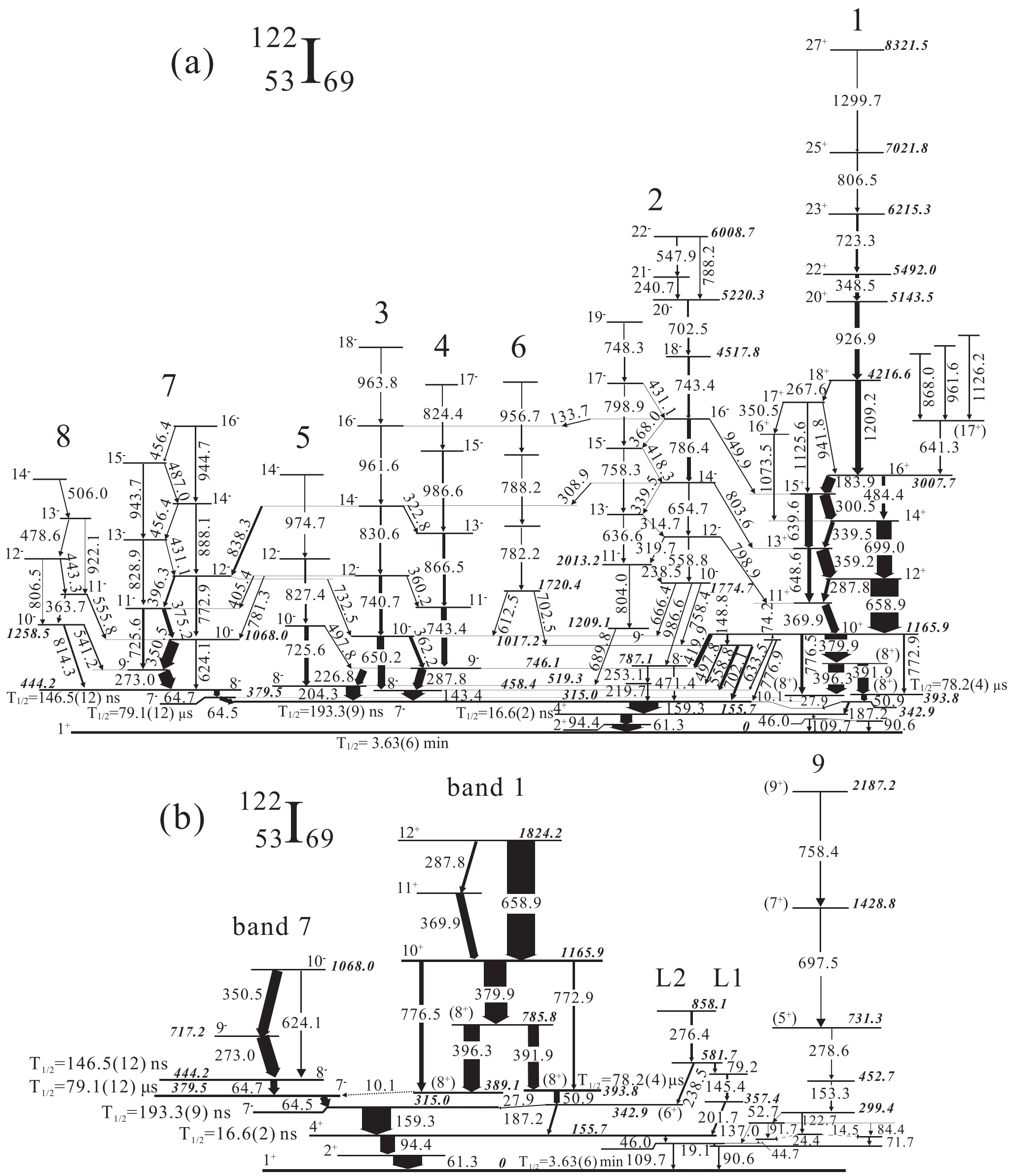

FIG. 4. Level scheme of ^{122}I deduced from the present work with the ^{120}Sn(^{7}Li, 5n)^{122}I reaction at $E_{\rm lab} = 58$ MeV. In (b) low-lying levels including the weakly populated positive-parity states are exhibited. The isomers identified in the present work are indicated by a half-life of $T_{1/2}$. Note that all energy values are corrected based on Table I.

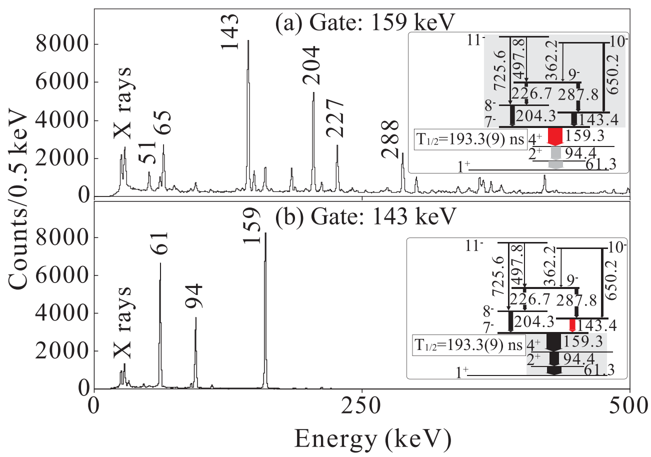

FIG. 6. Coincidence γ-ray spectra showing transitions occurring 80–900 ns before (early delayed) the gating 159-keV transition in (a) and 80–900 ns after (late delayed) the gating 143-keV transition in (b). Note that all energy values are corrected based on Table I.

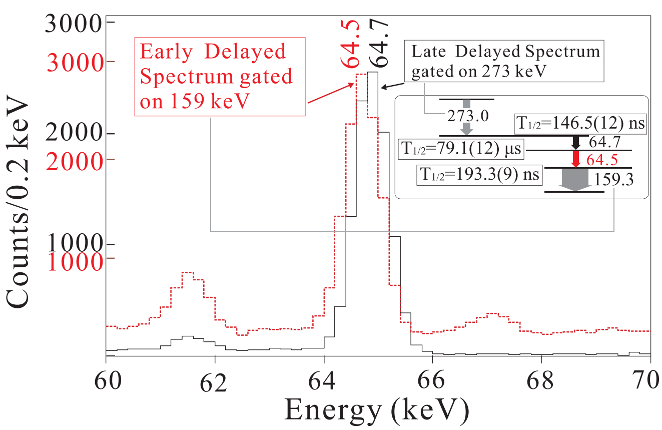

FIG. 9. Energy difference of a doublet 65-keV γ ray between the early-delayed spectrum by gating on the 159-keV transition and the late-delayed spectrum by gating on the 273-keV transition. Also see Fig. 4. Note that all energy values are corrected based on Table I.

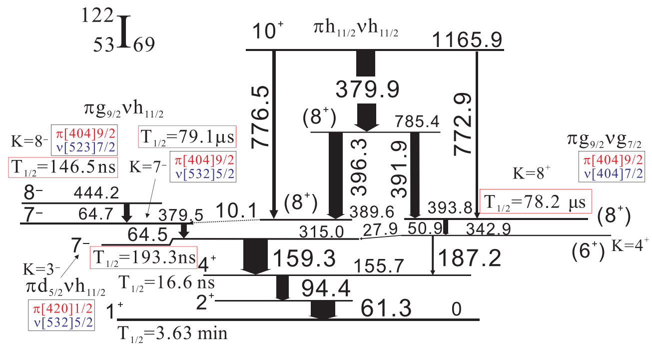

FIG. 19. The isomeric states identified in the present paper for ^{122}I. The corresponding proton-neutron shell configurations, Nilsson orbitals, and K-quantum numbers are indicated. Note that all energy values are corrected based on Table I.

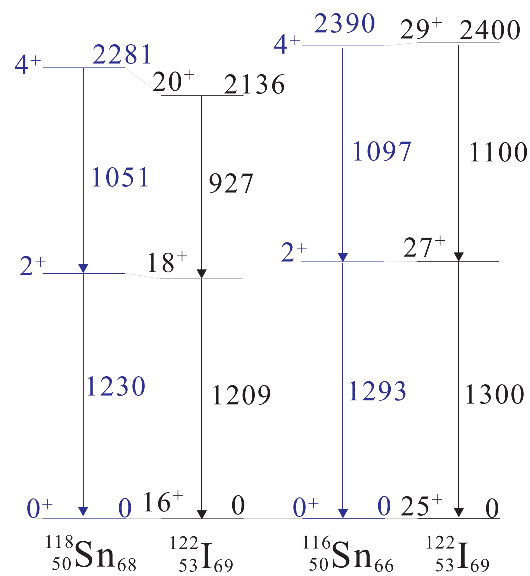

FIG. 24. Level comparisons between the ground band states of ^{118}Sn and the 20^+ to the 16^+ states of ^{122}I and the ground band states of ^{116}Sn and the 29^+ to 25^+ states of ^{122}I. Note that the referenced levels, 16^+ and 25^+ states for ^{122}I are all set to be zero in energy. Energies are given in keV. The transitions of 29^+ to 27^+ in ^{122}I are quoted from [12]. Note that a typographical error 907 keV is corrected as 927 keV.

[9] C.-B. Moon, G. D. Dracoulis, R. A. Bark, A. P. Byrne, P. A. Davidson, A. N. Wilson, T. Kibédi, and G. J. Lane, Department of Nuclear Physics Annual Report, ANU-P/1564, Australian National University, 2002, pp. 11–17.

[12] P. Singh, S. Nag, K. Selvakumar, A. K. Singh, I. Ragnarsson, A. Bisoi, A. Goswami, S. Bhattacharya, S. Kumar, K. Singh, J. Sethi, S. Saha, T. Trivedi, S. V. Jadhav, R. Donthi, B. S. Naidu, and R. Palit, Phys. Rev. C **85**, 054311 (2012).